

Encapsulation and release characteristics of Marigold oleoresin in chitosan grafted sodium acrylate-co-acrylamide

Shruthi. S. B¹, Pratik Roy¹, R. R. N. Sailaja^{1*}, Chandan Sengupta²

¹The Energy and Resources Institute (TERI), SRC, Bangalore 560071, India

²Department of Botany, University of Kalyani, Kalyani 741235, India

*Corresponding author. Tel: (+91) 080-25356590; E-mail: sailaja.bhattacharya@gmail.com

Received: 04 December 2015, Revised: 12 February 2016 and Accepted: 01 June 2016

ABSTRACT

Marigold oleoresin has been widely used in the pharmaceutical industry because of its medicinal properties. In this study, marigold oleoresin was encapsulated in chitosan grafted sodium acrylate-co-acrylamide. Emulsification process was used to prepare the beads containing marigold oleoresin and the grafted polymer was characterized using FTIR, SEM and TGA. The properties of the beads such as size, swelling characteristics, encapsulation efficiency and release kinetics were studied. The bead size was in the range of 0.46 to 1.05 mm. The antimicrobial activity and cyto-compatibility studies of marigold oleoresin were also conducted. The marigold oleoresin beads showed zero order release kinetics. Copyright © 2016 VBRI Press.

Keywords: Encapsulation; swelling characteristics; release kinetics; antimicrobial activity; cyto-compatibility.

Introduction

Calendula officinalis L. or pot marigold is a common garden plant belonging to the family asteraceae. *Calendula* is usually native to Southern European region including Italy, Malta, Greece, Turkey, Portugal, and Spain [1]. It is currently cultivated in many temperate regions of the world like India, depending on its commercial value. *Calendula* grows up to 50 cm in height and produces large yellow or orange flowers [2]. The flowers are the part of the herb used medicinally in the form of infusions, tinctures, liquid extracts, creams or ointments. Flower extract, flower essential oil and seed oil of *Calendula officinalis* L. are cosmetic constituents and the plant has been presented as a new source for cosmetic industry [3].

For centuries, calendula flowers have been used to treat a number of clinical conditions, specifically the treatment of dermatological disorders such as, acnes and burns [4, 5]. *Calendula* plant is listed in German Commission E, European Scientific Co-operative on Phytotherapy, British Herbal Pharmacopoeia and World Health Organization monographs for wound healing and anti-inflammatory actions [6]. The plant has been reported to contain mainly carotenoids, flavonoids, phenolic acids, and triterpenoids [7]. The main compounds within calendula are the triterpenoids which are claimed to be the most important anti-inflammatory and antioedematous components within the plant [8]. Other constituents identified in calendula such as flavonoids, essential oils and sesquiterpenes, may also be responsible for the antioedematous, anti-inflammatory, antioxidant, and wound healing effect of the plant [9]. Moreover, *in vitro* antimicrobial activity of the calendula extract has also been well documented [10]. Extracts from the plant have been described to show activity against

HIV-1 replication [11]. Studies revealed that calendula also possesses antiviral, antitumoral and antimutagenic properties [12]. *Calendula* have been found to be usually safe [13], although very rare occurrence of contact dermatitis due to Asteraceae plants has also been reported [14, 15].

In the present study, superabsorbent polymer based on chitosan grafted with sodium acrylate-co-acrylamide has been synthesized. Marigold oleoresin has been encapsulated with above mentioned chitosan based grafted superabsorbent polymer. Oleoresin containing beads has been characterized for swelling characteristics and encapsulation efficiency. Morphological characterization and thermal analysis of these beads have also been performed. The product thus developed has the potential to find application for healing minor external wounds. This would ensure that the active ingredients of the herbal oleoresin will be released over a prolonged period of time on a sustainable basis. Encapsulation using biocompatible antibacterial material rather than commonly used bio inert matrix would have the twin advantages of healing and prevention of wound infection. However, a study on this aspect is novel and not found in literature.

Experimental

Materials

The extracted marigold oleoresin (95% purity) of technical grade sample was obtained from M/s. Natsyn Catalysts, Tamilnadu, India. Chitosan powder used in this study was obtained from Marine Chemicals, Cochin (India) with 85 % deacetylation. Sodium acrylate (97 %) was procured from Sigma Aldrich, USA. Acrylamide, Methylene bisacrylamide, Ammonium persulfate, Methanol, Hexane

and other chemicals of analytical grade has been procured from S. D. Fine chemicals, Mumbai, India. All chemicals were used without further purification.

Grafting

The graft polymerization of acrylamide and sodium acrylate onto chitosan backbone was conducted as follows. 1g of chitosan was dissolved in 100 ml of 2 wt % acetic acids. Chitosan solution was hydrolyzed with 1N NaOH solution, and then 80 ml of NaOH was added to the hydrolyzed precipitate and stirred for 20 minutes. Following this, sodium acrylate and acrylamide were added in the ratio of 3:2 to the chitosan solution. The reaction mixture was then put in a locally fabricated microwave reactor (Enerzi microwave systems, Belgaum, India) at 70 °C, 0.8 kW for about 3 minutes and the reaction was initiated by the addition of known quantity of ammonium persulfate. Methylene bisacrylamide was used as cross linker in this reaction. The reaction product was taken out from the reactor and was cooled to room temperature. The mixture was neutralized to pH 7 by using 1N NaOH solution. The mixture was then precipitated using methanol. The precipitate obtained was kept for drying at 80 °C for 6 hours.

Preparation of beads

The grafted superabsorbent polymer was dissolved in 10 wt % acetic acid. To this solution, a known quantity of marigold oleoresin was mixed and stirred well and left to stand overnight to remove air bubbles. The above solution was then dropped into formaldehyde solution using a 25 ml hypodermic syringe having 1mm diameter with constant stirring for an hour. The beads thus formed were then crosslinked using 1 % (v/v) glutaraldehyde solution by stirring the beads in the solution for an hour. Later, the crosslinked beads were rinsed with distilled water and dried in air overnight.

Preparation of phosphate buffered saline (PBS)

Phosphate buffered Saline (PBS) was prepared by dissolving 8g of NaCl, 0.2g of KCl, 1.44g of Na₂HPO₄ and 0.24g of KH₂PO₄ in 800 ml of distilled water. Then pH of the solution was adjusted to 7.4 by using HCl. After that volume of the solution was made 1 liter by addition of distilled water. Finally, the solution was sterilized by using autoclave.

Characterization

Fourier transform infrared spectroscopy (FTIR)

The Fourier transform infrared spectroscopy (FTIR) analysis of pure chitosan and chitosan grafted sodium acrylate-co-acrylamide were carried out by using FTIR Spectrophotometer (Bruker ALPHA FT-IR Spectrometer) between 600 and 4000 cm⁻¹.

Bead size measurement

An average of 50 beads was completely dried and their sizes were measured by using standard digital Vernier calipers.

Scanning electron microscope (SEM)

The topographical characterization of the beads was carried out using a scanning electron microscope (SEM) (JEOL, JSM-840 microscope). The specimens were gold sputtered prior to microscopy.

Swelling kinetics of beads

Swelling of the beads was studied by the measurement of water uptake by the beads at particular time intervals. The study was carried out in acidic, basic and neutral medium for a period 4 hours. Known quantity of beads was initially taken in separate test tubes containing each medium. Then the mass of every individual bead was taken at different intervals of time and the average value was calculated. During this process care was taken in handling of the swollen beads so as to avoid mass loss by breaking or erosion of beads.

Content uniformity or encapsulation efficiency

Beads were evaluated for the marigold oleoresin content and this was done by refluxing a known mass of beads with 100 ml of hexane at 65 °C. Refluxing was continued to ensure the complete extraction of marigold oleoresin from the beads. Then the absorbance of hexane containing the extracted amount of marigold oleoresin was observed using a UV spectrophotometer (Lovibond PC SPECTRO, 666 HELMA (2265)) using hexane as blank. Encapsulation efficiency was determined from the following formula:

$$\text{Encapsulation efficiency (\%)} = \frac{(\text{Total amount of oleoresin} - \text{Free oleoresin})}{\text{Total amount of oleoresin}} \times 100$$

Release kinetics

The release kinetics of the beads containing marigold oleoresin was carried out by taking a known mass of beads in PBS and shaken well. At definite time intervals, the absorbance of PBS containing extracted marigold oleoresin was taken at a particular wavelength using UV Spectrophotometer (Lovibond PC SPECTRO, 666 HELMA (2265)). This procedure was carried out for a period of 4 hours. Further the modeling of oleoresin release from the swellable polymeric systems was analyzed using kinetic models.

Antimicrobial activity

The antibacterial activity of the marigold oleoresin was evaluated by the paper-disk agar diffusion method against the two Gram-negative pathogenic bacteria *Proteus mirabilis* (MTCC 9493), *Pseudomonas aeruginosa* (MTCC 1688) and one Gram-positive pathogenic bacteria *Staphylococcus aureus* (MTCC 3160). Microorganisms were obtained from Microbial Type Culture Collection and Gene Bank (MTCC) Chandigarh, India. Organisms were maintained on Muller-Hinton agar (MH). Inocula were prepared by diluting overnight (24hours, at 37 °C) cultures in Muller Hinton broth medium to approximately 10⁶ CFU/ml. Absorbent discs (Whatman disc No.3, 6 mm

diameter) were soaked with 10 μ l of oleoresin and then placed on the surface of inoculated Petri dishes (90 mm). Diameters of growth inhibition zones were measured after incubation at 37 °C for 24 hours. The experiment was carried out in triplicate.

In vitro cytotoxicity test

Cell line and culture medium

NIH 3T3 cells were procured from NCCS, Pune, India. NIH 3T3 cell line was cultured in Dulbecco's Modified Eagle Medium (DMEM) supplemented with 10 % inactivated Fetal Bovine Serum (FBS), penicillin (100 IU/ml), streptomycin (100 μ g/ml) and amphotericin B (5 μ g/ml) in an humidified atmosphere of 5 % CO₂ at 37 °C until confluent. The cells were dissociated with TPVG solution (0.2 % trypsin, 0.02 % EDTA, 0.05 % glucose in Phosphate Buffered Saline (PBS)). The stock cultures were grown in 25 cm² culture flasks and all experiments were carried out in 96 microtitre plates.

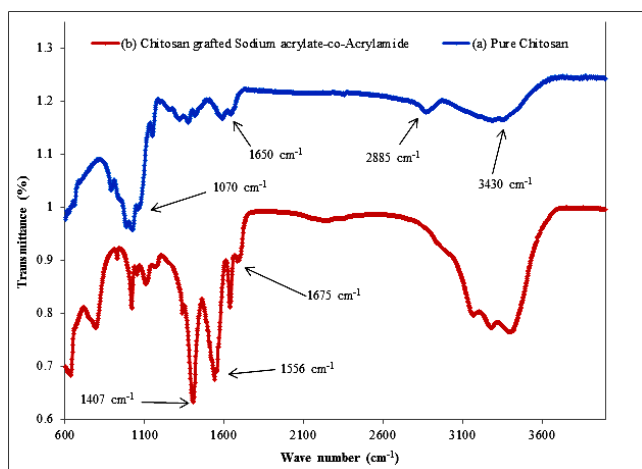


Fig. 1. FTIR spectrum of pure chitosan and chitosan grafted sodium acrylate-co-acrylamide.

Determination of cell viability by NRU assay

The monolayer cell culture was trypsinized/ scrapped with cell scrapper and the cell count was adjusted to 1.0 x 10⁵ cells/ml using DMEM containing 10 % FBS. To each well of the 96 well microtitre plate, 0.1 ml of the diluted cell suspension (approximately 10,000 cells) was added. After 24 hours, when a partial monolayer was formed, the supernatant was discarded and the monolayer was washed once with the culture medium. 100 μ l of different marigold oleoresin concentrations were added on to the partial monolayer in microtitre plates. The plates were then incubated at 37 °C for 24 hours in 5 % CO₂ atmosphere. The microscopic examination for these samples was carried out and observations were noted every 24 hours. After 24 hours, the marigold solutions in the wells were discarded and 50 μ g/ml of neutral red in PBS was added to each well. After 3 hours of culture, the medium was removed and the plate was rinsed 2 times with PBS. The desorbing solution (1 % glacial acetic acid, 50 % ethanol and 49 % H₂O) of 100 μ l to each well was added and shaken for 15 minutes. The absorbance of coloured solution was measured at 540 nm with a microplate reader. The concentration producing

50% inhibition for neutral red uptake (CTC₅₀) was calculated by following formula,

$$\% \text{ Growth Inhibition} = 100 - \left[\frac{\text{Mean OD of individual test group}}{\text{Mean OD of control group}} \times 100 \right]$$

Thermogravimetric analysis (TGA)

Thermogravimetric analysis (TGA) of pure chitosan and chitosan grafted sodium acrylate-co-acrylamide were carried by using Perkin-Elmer Pyris Diamond 6000 analyzer [Perkin Elmer Inc., USA] in a Nitrogen atmosphere. The samples were subjected to a heating rate of 10 °C/min in a heating range of 30 °C – 600 °C using Al₂O₃ as reference material.

Results and discussion

FTIR analysis

The FTIR spectrum of pure chitosan and chitosan grafted sodium acrylate-co-acrylamide is shown in **Fig. 1**. The FTIR spectrum of pure chitosan (curve-a) reveals characteristic peaks at 3430 cm⁻¹ which represents the stretching vibration of -O-H, while 1650 cm⁻¹ peak shows the characteristic peak of (C=O) amide I carbonyl stretching and the peaks from 1425 cm⁻¹ correspond to the -C-H symmetrical deformation. The peaks at 1070 and 2885 cm⁻¹ are related to (C-O-C) stretching vibration and aliphatic -C-H stretching vibration respectively [16, 17].

Curve-b depicts chitosan grafted sodium acrylate-co-acrylamide spectrum. The hydrogel comprised of a chitosan backbone with side chains that carry carboxamide and carboxylate functional groups, which are evidenced by 3 new peaks at 1407, 1556, and 1675 cm⁻¹ (Curve-b). These peaks are attributed to C=O stretching in the carboxamide functional groups, and symmetric and asymmetric stretching modes of the carboxylate groups, respectively [18]. The aforesaid three peaks do not exist in pure chitosan. The peak at 2885 cm⁻¹ for -CH stretching in pure chitosan spectrum is not seen in the chitosan grafted sodium acrylate-co-acrylamide indicating successful grafting of sodium acrylate-co-acrylamide with chitosan.

Bead size measurement

The average bead size measurement of marigold oleoresin beads was performed by using digital Vernier calipers and was found to be 0.76 mm for an average of 50 beads. The beads were having a size ranging between 0.46 mm to 1.05 mm.

SEM morphology

The SEM morphology of chitosan grafted sodium acrylate-co-acrylamide beads containing marigold oleoresin is shown in **Fig. 2**. The micrographs depict that beads formed were spherical in shape and had a rough and irregular surface.

Swelling characteristics of beads

The swelling behavior of chitosan grafted sodium acrylate-co-acrylamide beads containing marigold oleoresin is shown in **Fig. 3** and **Table 1**. It can be observed that beads

show more swelling in neutral and acidic medium than compared to basic medium (Fig. 3).

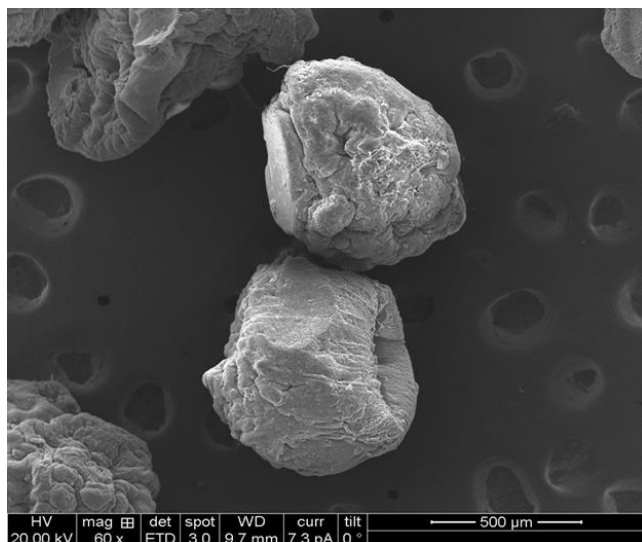


Fig. 2. SEM micrograph showing surface morphology of chitosan grafted sodium acrylate-co-acrylamide beads containing marigold oleoresin.

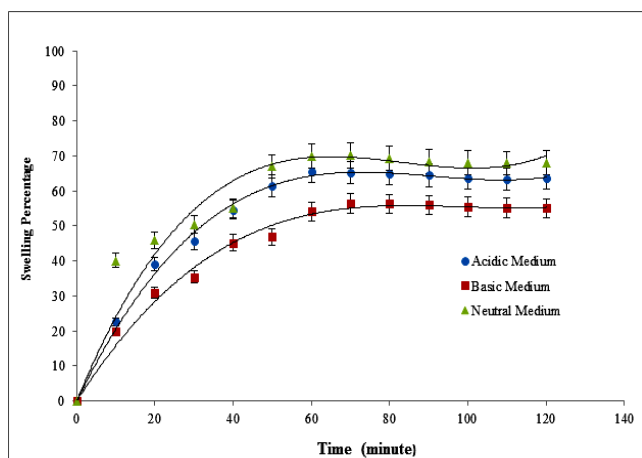


Fig. 3. Swelling study of marigold oleoresin beads in acidic, basic and neutral buffer.

Table 1. Swelling percentage of chitosan grafted sodium acrylate-co-acrylamide beads in different mediums.

Buffer used	Acidic	Basic	Neutral
Marigold oleoresin beads swelling percentage (%)	65.62%	56.4%	70.1%

Fig. 3 and Table 1 show the swelling behaviors of chitosan grafted superabsorbent co-polymeric beads. As seen in Table 1, neutral medium exhibits maximum swelling followed by swelling in acidic medium. The beads show that least swelling in basic medium. It has been envisaged that at both low and high pH, the concentrations of ions are high which cause an increase in ionic strength. When the ionic strength is increased, the difference in osmotic pressure between the inside and outside of the beads is reduced thereby, leading to reduction in swelling capabilities. Similar behavior in various natural polysaccharide hydrogels has been observed by Sorur *et al.* [19].

Content uniformity or encapsulation efficiency

The chitosan grafted sodium acrylate-co-acrylamide beads containing marigold oleoresin were evaluated for its encapsulation efficiency using UV spectrophotometer. In the preliminary trials, the beads were loaded with different amounts of oleoresin and it was observed that 200 mg of oleoresin loading for 100 ml of the grafted material was optimum. The encapsulation efficiency for the above formulation was found to be 75.7 %.

Table 2. The order release constants and the n values of marigold oleoresin.

Zero order	First order	Higuchi	Power law/ Korsmeyer-Peppas model
$k_0=0.42$	$k_1=0.0021$	$k_H=7.49$	$k=0.51$
$R^2=0.99$	$R^2=0.72$	$R^2=0.90$	$R^2=0.96$
			$n=0.95$

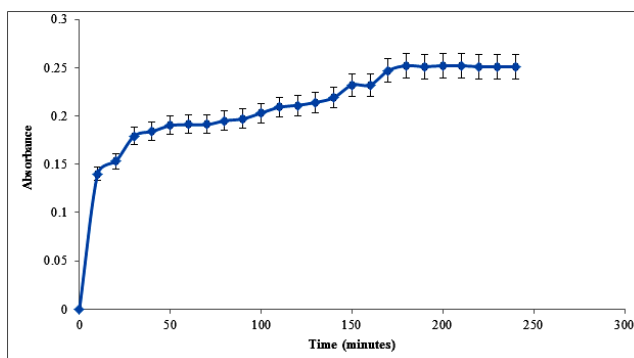


Fig. 4. Release behavior of chitosan grafted sodium acrylate-co-acrylamide beads containing marigold oleoresin.

Release kinetics

The release of marigold oleoresin from the swellable polymeric systems has been analyzed using mathematical models given below [20].

$$\text{Zero order: } \frac{M_t}{M_\infty} = k_0 t \quad (a)$$

$$\text{First order: } \frac{M_t}{M_\infty} = 1 - \exp(-k_1 t) \quad (b)$$

$$\text{Higuchi model: } \frac{M_t}{M_\infty} = k_H t^{\frac{1}{2}} \quad (c)$$

$$\text{Power model (or) Korsmeyer-Peppas model: } \frac{M_t}{M_\infty} = k t^n \quad (d)$$

where, M_t/M_∞ is the fractional release of drug in time t , ' k_0 ', ' k_1 ', ' k_H ' and ' k ' represent zero-order release constant, first order release constant, Higuchi constant and Korsmeyer-Peppas constant of the drug polymer system respectively, ' n ' is the diffusion exponent characteristic of the release mechanism. The values of ' n ', ' k_0 ', ' k_1 ', ' k_H ' and ' k ' were evaluated using equations (a) to (d) for the release kinetics of marigold oleoresin from the chitosan grafted sodium acrylate-co-acrylamide beads and the results are presented in the Table 2.

Using the least squares procedure, we have estimated the values of n and k for the present system. From the results obtained [Fig. 4(a, b, c and d)], we can see that zero order release model and Korsmeyer-Peppas model fits better compared to other two models. The zero order rate equation describes the systems where the release rate is

independent of its concentration while the Korsmeyer-Peppas model is often used to describe the release behavior from polymeric systems. The diffusional exponent, n , is dependent on the geometry of the device as well as the physical mechanism for release.

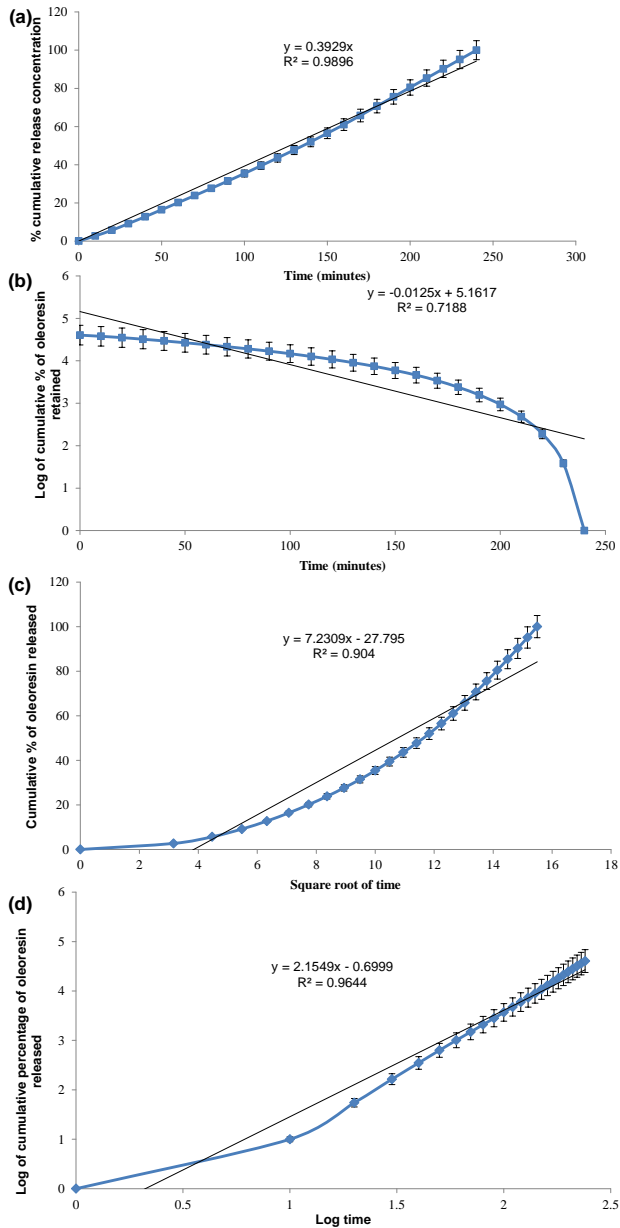


Fig. 4. (a). Zero order release model of marigold oleoresin sustained release formulation, (b) First order release model of marigold oleoresin sustained release formulation, (c) Higuchi release model of marigold oleoresin sustained release formulation and (d) Power law model for mechanism of marigold oleoresin sustained release formulation.

The values of n for a spherical device are 0.45 for Fickian release, 0.89 for case II (zero-order release) transport and > 0.89 for super case II transport in this model. For systems exhibiting super case II transport, the dominant mechanism for drug transport is due to polymer matrix relaxation. The value of $n > 0.45$ but < 0.85 is considered as anomalous transport (non-Fickian) and refers to the coupling of Fickian diffusion and relaxation of entangled chains of the encapsulating polymer. The first order model and Higuchi model describes the release from

system where release rate is concentration dependent and the release of drugs from insoluble matrix as a square root of time dependent process based on Fickian diffusion respectively [21, 22]. Since the R^2 value of 0.99 of zero order release model is the highest as compared to that of other models, it can be said that the release of oleoresin from the encapsulated beads maybe independent of its initial concentration. This suggests that the release characteristic of marigold oleoresin follows zero order kinetics.

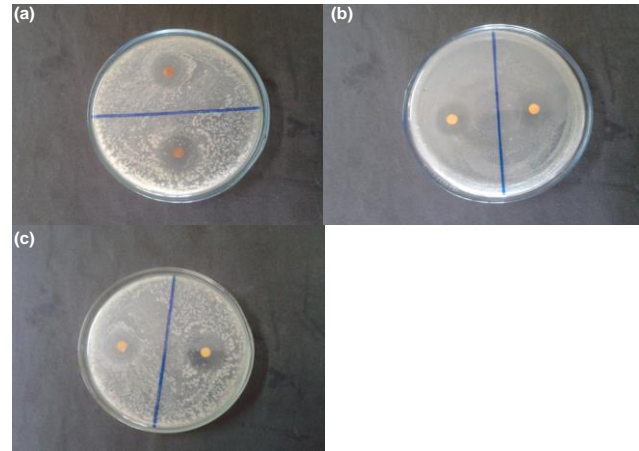


Fig. 5. Antimicrobial activity of marigold oleoresin against (a) *Pseudomonas aeruginosa*, (b) *Proteus mirabilis* and (c) *Staphylococcus aureus*.

Table 2. (a). Showing zone of inhibition of marigold oleoresin against three pathogenic bacteria.

Name of the pathogen	Trial 1	Trial 2	Trial 3	Mean diameter (mm)
<i>Proteus mirabilis</i>	19.1	18.7	19.6	19.13±0.45
<i>Staphylococcus aureus</i>	18.1	18.7	19.9	18.9±0.92
<i>Pseudomonas aeruginosa</i>	16.8	15.1	15.3	15.73±0.93

Antimicrobial activity

In the present investigation marigold oleoresin (10 μ l per disc) was tested for their putative antibacterial activity against three model bacteria. Paper-disk agar diffusion method was used to determine the zone of inhibition of bacterial growth. Efstratiou *et al.* [23] showed antibacterial activity of floral part extracts of marigold against both Gram-positive and Gram-negative pathogenic bacteria. Similar observation on the antibacterial activity of marigold oleoresin has been displayed against both Gram-positive and Gram-negative pathogenic bacteria. Results showed that marigold oleoresin was most active against *Proteus mirabilis* (Table 2(a), Fig. 5) with inhibition zones ranging from 18.7 mm to 19.6 mm (mean value: 19.13 \pm 0.45 mm). The mean diameter of the inhibition zone for *Staphylococcus aureus* was 18.9 \pm 0.92 mm. The smallest zone was recorded for *Pseudomonas aeruginosa* (mean diameter: 15.73 \pm 0.93 mm).

In vitro cytotoxicity test

NRU assay

Biocompatibility of marigold oleoresin was examined by NRU assay. Cytotoxicity in this assay is expressed as a

concentration-dependent reduction of the uptake of the vital dye Neutral Red (NR) when measured 24 hours after treatment with the test chemical and irradiation. NR is a weak cationic dye that readily penetrates cell membranes by non-diffusion, accumulating intracellularly in lysosomes. Alterations of the cell surface of the sensitive lysosomal membrane lead to lysosomal fragility and other changes that gradually become irreversible. Such changes brought about by the action of xenobiotics result in a decreased uptake and binding of NR. It is thus possible to distinguish between viable, damaged or dead cell, which is the basis of this test [24]. In this study NIH 3T3 cell line was examined for cytotoxicity of varied concentration of marigold oleoresin. **Fig. 6** shows the percentage of cytotoxicity for NIH 3T3 cell line. Cytotoxicity percentage increased 58.26% by increasing the concentration of marigold oleoresin from 62.5 µg/ml to 125 µg/ml. However, for higher concentration of marigold oleoresin specimen i.e. 500 µg/ml and 1000 µg/ml the rise in cytotoxicity percentage is only 10.93%. Marigold oleoresin specimen was found to be nontoxic against NIH 3T3 cell line with CTC₅₀ showing more than 1000 µg/ml value. Based on the above result it can be deduced that the marigold oleoresin specimen is cytocompatible.

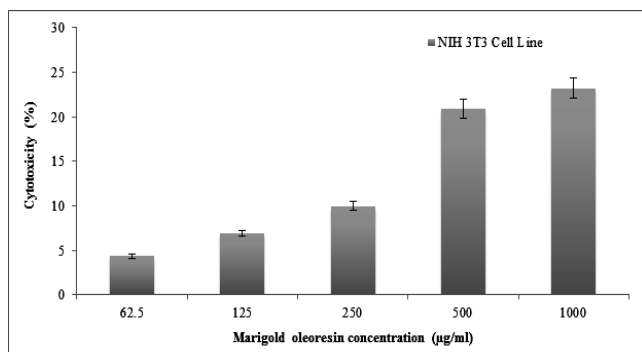


Fig. 6. Cytotoxicity of marigold oleoresin against 3T3 cell line by NRU assay (data are presented as the means \pm 2 standard deviation).

Thermogravimetric analysis (TGA)

Fig. 7 shows the TGA thermograms of neat chitosan and grafted chitosan. It can be clearly seen the grafting enhanced the thermal stability as grafted chitosan has higher thermal stability than neat chitosan.

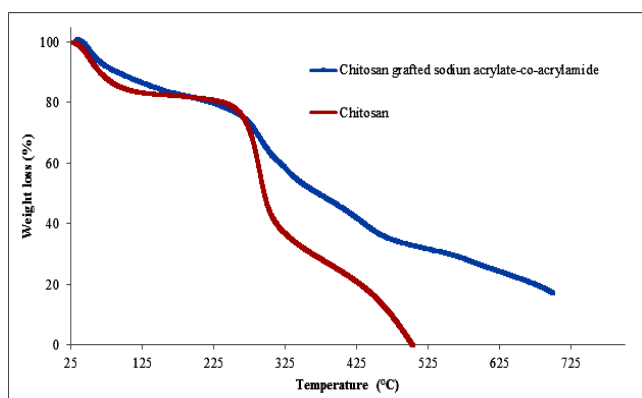


Fig. 7. TGA thermograms of pure chitosan and chitosan grafted sodium acrylate-co- acrylamide.

Conclusion

In the present study, marigold oleoresin has been encapsulated in grafted chitosan beads. The encapsulated beads were observed to have an encapsulation efficiency of 75.7%. SEM micrographs of beads revealed spherical shape with rough and irregular surface. These beads were studied for swelling characteristics in the different mediums and it was observed that the grafted beads showed maximum swelling in neutral medium. The release behavior followed zero order kinetics with a R^2 value of 0.99. Marigold oleoresin showed a good antimicrobial activity and it is non-cytotoxic. From this study it has been observed that marigold oleoresin encapsulated beads show an active controlled release system thereby indicating that they can be used in external wound dressing application for minor superficial wounds. This study can be further expanded for large scale production. In addition, another antifungal material can be included along with marigold oleoresin to enhance wound healing and protection against secondary infection.

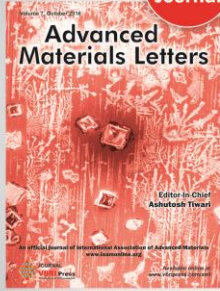
Acknowledgements

The authors are grateful to Department of Science and Technology (Green Chemistry Program), Government of India for kindly sanctioning funds to carry out this research work.

References

- Rejskova, A.; Brom, J.; Pokorny, J.; Korec'ko; *J. Flora.*, **2010**, *205*, 282.
DOI: [10.1016/j.flora.2009.05.001](https://doi.org/10.1016/j.flora.2009.05.001)
- Muley, B. P.; Khadabadi, S.S.; Banarase, N.B; *Trop. J. Pharm. Res.* **2009**, *8*, 455.
DOI: [10.4314/tjpr.v8i5.48090](https://doi.org/10.4314/tjpr.v8i5.48090)
- Andersen, F. A.; Bergfeld, W. F.; Belsito, D.V.; Hill, R. A.; Klaassen, C. D.; Liebler, D. C.; Marks Jr, J. G.; Shank, R. C.; Slaqa, T. J.; Snyder, P. W; *Int. J. Toxicol.*, **2010**, *35*, 129.
DOI: [10.1177/1091581810384883](https://doi.org/10.1177/1091581810384883)
- Bedi, M. K.; Shenefelt, P. D., *Arch. Dermatol.* **2002**, *138*, 232.
DOI: [10.1001/archderm.138.2.232](https://doi.org/10.1001/archderm.138.2.232)
- Fronza, M.; Heinzmann, B.; Hamburger, M.; Laufer, S.; Merfort, I; *J. Ethnopharmacol.*, **2009**, *126*, 463.
DOI: [10.1016/j.jep.2009.09.014](https://doi.org/10.1016/j.jep.2009.09.014)
- Arora, D.; Rani, A.; Sharma, A; *Pharmacogn. Rev.*, **2013**, *7*, 179.
DOI: [10.4103/0973-7847.120520](https://doi.org/10.4103/0973-7847.120520)
- Kishimoto, S.; Maoka, T.; Sumitomo, K.; Ohmiya, A; *Biosci. Biotechnol. Biochem.*, **2005**, *69*, 2122.
DOI: [10.1271/bbb.69.2122](https://doi.org/10.1271/bbb.69.2122)
- Loggia, R.D.; Tubaro, A.; Sosa, S.; Becker, H.; Saar, St.; Isaac, O; *Planta. Med.*, **1994**, *60*, 516.
DOI: [10.1055/s-2006-959562](https://doi.org/10.1055/s-2006-959562)
- Danielski, L.; Campos, L.M.A.S.; Bresciani, L.F.V.; Hense, H.; Yunes, R. A.; Ferreira, S.R.S; *Chem. Eng. Process.*, **2006**, *46*, 99.
DOI: [10.1016/j.cep.2006.05.004](https://doi.org/10.1016/j.cep.2006.05.004)
- Herman, A.; Herman, A. P.; Domagalska, B. W.; Mlynarczyk. A; *Indian. J. Microbiol.*, **2012**, *53*, 232.
DOI: [10.1007/s12088-012-0329-0](https://doi.org/10.1007/s12088-012-0329-0)
- Kalvatchev, Z.; Walder, R.; Garzaro, D; *Biomed. Pharmacother.*, **1997**, *51*, 176.
DOI: [10.1016/S0753-3322\(97\)85587-4](https://doi.org/10.1016/S0753-3322(97)85587-4)
- Barajas-Farias, L.M.; Perez-Carreón, J.I.; Arce-Popoca., E.; Fattel-Fazenda, S.; Aleman-Lazarini, L.; Hernandez-Garcia, S.; Salcido-Neyoy, M.; Cruz-Jimenez, F.G.; Camacho, J.; Villa-Trevino, S; *Planta. Med.*, **2005**, *71*, 1.
DOI: [10.1055/s-2005-916196](https://doi.org/10.1055/s-2005-916196)

13. Andersen, F.A.; Bergfeld, W.F.; Belsito, D.V.; Hill, R.A.; Klaassen, C.D.; Liebler, D.C.; Marks, Jr. J.G.; Shank, R.C.; Slaga, T.J.; Snyder, P.W; *Int. J. Toxicol.*, **2010**, 29, 221.
DOI: [10.1177/1091581810384883](https://doi.org/10.1177/1091581810384883)
14. Reider, N.; Komericki, P.; Hausen, B.M.; Fritsch, P.; Aberer, W; *Contact. Dermatitis.*, **2001**, 45, 269.
DOI: [10.1034/j.1600-0536.2001.450503.x](https://doi.org/10.1034/j.1600-0536.2001.450503.x)
15. Paulsen, E; *Contact. Dermatitis.*, **2002**, 47, 189.
DOI: [10.1034/j.1600-0536.2002.470401.x](https://doi.org/10.1034/j.1600-0536.2002.470401.x)
16. Thein-Han, W.W.; Misra, R.D.K; *Acta. Biomater.*, **2009**, 5, 1182.
DOI: [10.1016/j.actbio.2008.11.025](https://doi.org/10.1016/j.actbio.2008.11.025)
17. Xianmiao, C.; Yubao, L.; Yi, Z.; Li, Z.; Jidong, L.; Huanan, W; *Mater. Sci. Eng. C. Mater. Biol. Appl.*, **2009**, 29, 29.
DOI: [10.1016/j.msec.2008.05.008](https://doi.org/10.1016/j.msec.2008.05.008)
18. Silverstein, R.M.; Webster, F.X. (Eds.); *Spectrometric Identification of Organic Compounds*; Wiley: USA, **1998**.
DOI: [10.1002/\(SICI\)1097-458X\(199911\)37:1](https://doi.org/10.1002/(SICI)1097-458X(199911)37:1)
19. Sorour, M.; Ei-Sayed, M.; El-Moneem, N.A.; Talaat, H.A.; Shalaan, H.; El-Marsafy, S; *Starch.*, **2013**, 65, 172.
DOI: [10.1002/star.201200108](https://doi.org/10.1002/star.201200108)
20. Das, R.K.; Kasoju, N.; Bora, U; *Nanomed. Nanotech. Biol. Med.*, **2010**, 6, 153.
DOI: [10.1016/j.nano.2009.05.009](https://doi.org/10.1016/j.nano.2009.05.009)
21. Fu, Y.; Kao, W. J.; *Expert. Opin. Drug. Deliv.*, **2013**, 4, 97.
DOI: [10.1517/17425241003602259](https://doi.org/10.1517/17425241003602259)
22. Sahoo, S.; Chakraborti, C.K.; Mishra, S. C.; *J. Adv. Pharm. Res.*, **2011**, 4, 2268.
DOI: [10.4103/2231-4040.85541](https://doi.org/10.4103/2231-4040.85541)
23. Efstratiou, E.; Hussain, A.I.; Nigam, P.S.; Moore, J.E.; Ayub, M.A.; Rao, J. R; *Complement. Ther. Clin. Pract.*, **2012**, 24, 1.
DOI: [10.1016/j.ctcp.2012.02.003](https://doi.org/10.1016/j.ctcp.2012.02.003)
24. Borenfreund, E.; Puerner, J. A; *Toxicol. Lett.*, **1985**, 24,119.
DOI: [10.1016/0378-4274\(85\)90046-3](https://doi.org/10.1016/0378-4274(85)90046-3)



A Monthly Journal

Advanced Materials Letters


Editor in Chief
Ashutosh Tiwari

Copyright © 2016 VBRI Press AB, Sweden

Publish your article in this journal

Advanced Materials Letters is an official international journal of International Association of Advanced Materials (IAAM, www.iaamonline.org) published monthly by VBRI Press AB from Sweden. The journal is intended to provide high-quality peer-review articles in the fascinating field of materials science and technology particularly in the area of structure, synthesis and processing, characterisation, advanced-state properties and applications of materials. All published articles are indexed in various databases and are available download for free. The manuscript management system is completely electronic and has fast and fair peer-review process. The journal includes review article, research article, notes, letter to editor and short communications.

www.vbripress.com/aml



VBRI Press
Commitment to Excellence